Wetting Behavior in Colloid−Polymer Mixtures at Different Substrates

Willem K. Wijting,* Nicolaas A. M. Besseling, and Martien A. Cohen Stuart

Laboratory of Physical Chemistry and Colloid Science, Wageningen University, P. O. Box 8038, 6700 EK Wageningen, The Netherlands

Received: April 16, 2003; In Final Form: July 23, 2003

We present experimental observations on wetting phenomena in depletion interaction driven, phase separated colloidal dispersions. The contact angle of the colloidal liquid−gas interface at a solid substrate was determined for a series of compositions. Upon approach to the critical point, a transition occurs from partial to complete wetting. The interaction with the substrate was manipulated by modifying the substrate with a polymer. In that case, a transition from partial to complete drying is observed upon approach to the critical point.

1. Introduction

Colloidal systems have played an important role as experimental model systems to study generic properties of fluid and solid matter in general.[1] In colloidal systems, time and length scales are larger than in molecular systems, so colloidal systems are in some respects more convenient in experimental studies. Another advantage of colloidal systems as compared to molecular systems is that we can tune the properties, such as particle size and the range and strength of the interactions, on a continuous scale. This motivates our use of colloidal systems as an experimental model system to investigate wetting phenomena.

The phase behavior in colloidal systems can be controlled by nonadsorbing polymer. Nonadsorbing polymer in a colloidal suspension of hard spherical particles yields an attractive contribution to the interaction between the particles, which is called depletion interaction.[1−10] The free energy of this depletion interaction is equal to the overlap volume of two depletion zones times the osmotic pressure because of the polymer. Below the polymer overlap concentration, the range of the attraction is twice the radius of gyration of the polymer. So the interaction can be tuned in both range and strength by varying the molecular mass and the concentration of polymer, respectively. If the concentrations of colloidal particles and polymer are sufficiently high, the depletion interaction will lead to phase separation: a colloid poor phase which is called *colloidal gas*, and a colloid rich phase, which is called *colloidal liquid*, coexist. Also a *colloidal crystal* may occur. Structure and phase behavior of colloidal systems is quite similar to that of systems consisting of noble gas atoms or simple isometric molecules. For several colloidal systems the phase behavior has been investigated both experimentally and theoretically.[1,4−7,11]

In the theories of Poon and Lekkerkerker,[5,6] the polymers are assumed to be ideal. This implies that (i) swelling of polymer because of interchain excluded volume interactions is ignored, (ii) the range of the depletion interaction is assumed independent of solvent quality and polymer concentration, and (iii) the polymer osmotic pressure is assumed to be given by the law of Van't Hoff. In experimental studies, the polymers are rarely ideal and the polymer concentration often exceeds the overlap concentration. Furthermore, in several older theories,[1,4−6] the interaction between two colloidal particles is taken to be pair wise additive. However, three and more body interactions are usually not negligible. Brader and others accounted for this nonpair wise additivity.[8,9,11] Aarts et al. made theoretical calculations in which excluded-volume polymer chains are explicitly considered.[11] In that paper, also the variation of the thickness of the depletion layer as a function of the curvature of the colloidal particles and of the concentration of polymer are taken into account.

The size ratio of the polymer coils and the colloidal particles ($q = R_g/R_c$, with R_g the radius of gyration of the polymer and R_c the radius of the colloidal particles) has to be $q > 0.3$ in order to make the existence of a colloidal liquid-state possible.[1,5,6] Generally, for a liquid phase to be possible an attraction with a range of the order of magnitude of the particles is required.

In this paper, we describe wetting experiments on phase separated colloid−polymer systems. We consider a solid substrate in equilibrium with two fluid phases (colloidal liquid and colloidal gas). In this situation, the equilibrium wetting state can be described by the static contact angle, θ_0. Through Young's law the contact angle is related to the interfacial tensions, γ[12]

$$\cos\theta_0 = \frac{\gamma_{SG} - \gamma_{SL}}{\gamma_{LG}} \tag{1}$$

Here, the subscripts S, L, and G refer to the solid substrate, the (colloidal) liquid, and the (colloidal) gas phases, respectively. If $0° < \theta_0 < 180°$ the substrate is said to be partially wet. Complete wetting corresponds with $\theta_0 = 0°$. In this case there can be no substrate−gas interface at coexistence of liquid and gas because a liquid film intervenes between the substrate and the gas phase. If $\theta_0 = 180°$, we speak of complete drying: at liquid−gas coexistence, a gas film will intervene between the liquid and the substrate.[13] γ_{LG} only depends on the interactions between the particles that make up the liquid and the gas phases, whereas γ_{SG} and γ_{SL} also depend on the interactions between these particles and the substrate.

Cahn predicted that, always when two coexisting fluid phases exist in the presence of a third phase (substrate), near the critical point, a substrate is completely wet by one of the two coexisting fluid phases. At a certain temperature below the critical point,

* To whom correspondence should be addressed.

10.1021/jp035019d CCC: $25.00
Published on Web 08/23/2003

wetting may change from complete to partial. This phenomenon is called the wetting transition and is a true phase transition.[14] If the derivative of a free energy-temperature curve (or a contact angle-temperature curve) is discontinuous at the wetting transition, a wetting transition is first order. If that derivative is continuous in the transition point, the transition is second order or critical.[15,17,18] First order wetting transitions occur usually far from the critical point, whereas second-order wetting transitions occur more close to the critical point.[17]

In nonequilibrium situations, the three phase contact line may move with respect to the substrate. Usually, the contact angle depends on the velocity with which the substrate and the contact line move with respect to each other. A liquid can advance over the substrate, or it can recede from the substrate, leading to advancing and receding contact angles, respectively. Extrapolation to zero velocity yields the static advancing and the static receding contact angle, respectively. For many systems, the static receding contact angle is smaller than the static advancing contact angle. So, at zero velocity, there is a discontinuity in a contact angle-velocity curve (contact angle hysteresis). This hysteresis occurs because of chemical inhomogeneity and/or roughness on the scale of molecules.[16]

The past 25 years have seen a revival of the study of fundamental aspects of wetting phenomena in general and wetting transitions in particular.[13−19] To investigate the relations between macroscopic wetting behavior and the underlying microscopic interactions, it would be convenient to have an experimental system in which these microscopic interactions can be tuned. With atomic or molecular systems, this is not possible. However, using colloidal systems, we can independently tune the interactions between the particle and that between a particle and the substrate and investigate the consequences for wetting behavior. Recently we published a letter on our first observations of a wetting transition in a phase separated colloid polymer mixture.[10] Furthermore Aarts et al. reported observations on menisci of the colloidal liquid−gas interface at a hard substrate.[20] In the present paper, we give a more elaborate account of wetting transitions in colloidal systems. We will vary the composition of colloid−polymer mixtures and study the wetting behavior as a function of the proximity to the critical point and investigate whether there is a wetting transition as predicted by Cahn.[15] We will also vary the interaction of the particles with the substrate by modifying the substrate. Although we will use dynamical experiments to determine contact angles, in the present paper, we will focus on static wetting behavior. Dynamic aspects will be discussed thoroughly in a subsequent paper.

2. Experimental Section

2.1. Colloidal System. We prepared colloidal particles by modifying commercially available silica particles (Ludox HS40, Aldrich) with stearyl alcohol (pA quality, Aldrich) using the method of van Helden and Pathmamanoharan.[21,22] The radius of these particles, dispersed in cyclohexane (pA quality, Aldrich), is $R_c = 14$ nm (determined by dynamic light scattering). The density of these particles is determined at 1.63×10^3 kg m^{-3} by weighing 5 mL of the dispersion, drying the dispersion, and weighing the dried particles. The refractive indices of silica and cyclohexane are very similar (1.4588 and 1.4266, respectively), so the van der Waals attraction between the particles is negligibly small and, in the absence of polymer, the particles behave as hard spheres.[21,23,24] Because of the low refractive index differences and the small size of the particles, even concentrated suspensions are transparent.

As nonadsorbing polymer, we used poly(dimethylsiloxane) (PDMS, Polymer Sources, Inc.) with a number average molecular weight, M_N, of 83 200 g/mol, corresponding to a radius of gyration, $R_g = 13$ nm. The heterodispersity index (M_W/M_N with M_W the weight average molecular mass) was 1.24. The radius of gyration was determined by extrapolation using the experimental data of Verhaegh, Bodnár, and de Hoog[25,26,27] and the scaling relation for a good solvent $R_g \propto M_N^{0.6}$.[28] That the latter relation applies for the present polymer solvent combination is confirmed by the experimental data.

The size ratio for our system $q = 0.93$. This is slightly lower than that of Verhaegh, de Hoog, and Aarts.[25,27,20] The liquid−gas phase behavior of similar silica/PDMS/cyclohexane systems has been studied extensively.[25−27]

We determined the phase diagram for our system by using the method of Bodnár and Oosterbaan, which requires the phase volumes along at least three different dilution lines (i.e., lines with a constant polymer-colloid concentration ratio) to be measured.[26,27] Using the mass balance, the phase diagram can be constructed. We used four dilution lines to get a higher accuracy.

2.2. Wetting Experiments. Contact angle measurements on the chosen colloidal liquid−gas system bring their own specific difficulties. One of the reasons is that the capillary length, l_c, is very small. The capillary length is defined by $l_c = (\gamma_{LG}/\Delta\rho g)^{1/2}$ (where $\Delta\rho$ is the density difference between the two fluid phases and g the gravitation constant). It determines the cross over between the regime where gravity dominates the shape of a meniscus and the regime where the interfacial tension dominates that shape. Here l_c is small (O tens of μm) because γ_{LG} in colloidal systems is very low (O μN m^{-1}),[27] whereas there is still an appreciable density difference. So, the menisci are very small. In typical molecular systems (far from the critical point), $l_c \sim O$ mm. We observed menisci at fibers with a diameter of about 0.2 mm, which were vertically suspended through the colloidal liquid−gas interface. The other difficulty is that the optical contrast between the two colloidal phases is low, which makes observations with a microscope rather difficult. We performed the wetting experiments using home-built viewing optics. The best results were obtained by illuminating the sample with a diffuse parallel light beam through the sample in the direction of objective and CCD Camera (Pulnix). The light beam was made parallel with the help of a negative lens ($f = -5.0$ mm, Ø = 5.0 mm) and a positive lens ($f = 70.0$ mm, Ø = 60 mm). A diffuse filter and a diaphragm were placed between the positive lens and the sample. The objective (Melles Griot) has a long working distance and a magnification of 15.75.

To determine dynamic contact angles, the fiber was moved through the interface at different velocities by means of an electronically controlled actuator (Newport). This actuator can move a plastic spring to which the fiber is attached. By moving the fiber downward, the liquid advances over the substrate, and by moving the fiber upward, the liquid recedes from the substrate. The fiber was moved into or out of the interface with velocities in the range of 0 to 15 μm s^{-1}. For each velocity, an image was captured 25 s after the beginning of the movement. After each experiment, we waited until the system was completely relaxed before starting a next measurement at another velocity. From the response of the meniscus to the movement of the fiber, we could distinguish the meniscus from its mirror image. Static contact angles were determined by interpolating the cosine of the contact angle to zero velocity. That such an interpolation is justified will be explained in the results section.

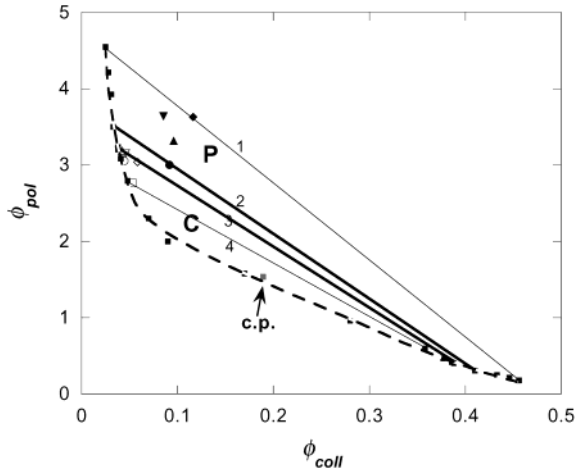

Figure 1. Phase diagram of the silica/PDMS/cyclohexane system. The polymer concentration, ϕ_{pol}, is plotted versus the volume fraction colloid ϕ_{coll}. The binodal points are denoted with solid squares and the critical point is indicated with c.p. The binodal is represented by the dashed curve. At the tielines (solid lines), indicated by 1, 2, 3, and 4, the polymer reservoir concentrations are 5.5, 4.5, 4.3, and 4.1, respectively. The overall compositions of the samples, used in the wetting experiments, are given by A (◆), B (▼), C (▲), D (●), E (◇), F (▽), G (△), H (○), J (□). Points E and G are on the same tieline (have the same polymer chemical potential). The complete and partial wetting regimes are indicated by C and P, respectively.

2.3. Substrates. In this paragraph, the preparation of the substrates is described. We examined two distinctly different substrates. One might be denoted *hard* substrate and the other *soft* substrate. The surface of a stearylated glass fiber should be similar to that of the colloidal particles and has only hard repulsion and depletion attraction with the particles. These are the hard fibers.

To prepare these, glass fibers were cleaned by ultrasonicating them for 30 min in ethanol (96%) and putting them in a plasma cleaner (Harrick PDC-32G) for 10 min at high RF level. The fibers were then stored for at least 24 h in clean ethanol (96%). This was done because we have indications that siloxane groups on the surface have to rehydrolyze after the plasma treatment. The fibers were coated with stearyl alcohol by heating them for 4 h in a melt of stearyl alcohol at 180 °C. After the heating procedure, the excess stearyl alcohol was removed from the fibers by storing the samples in chloroform. After at least 24 h, the fibers were stored in clean chloroform, before using them in experiments.

A second series of fibers were modified by grafting with PDMS (Aldrich $M_N = 31\,300$ and $M_W/M_N = 3.0$). To this end, they were heated, after the cleaning step, for 30 min at 70 °C in a melt of PDMS. After the heating procedure, excess PDMS was removed by storing the fibers in cyclohexane. After 24 h, the fibers were stored in clean cyclohexane. These fibers are denoted as *soft fibers*. That PDMS is attached to the glass can be deduced from the observations that the contact angle of water is significantly larger on a PDMS treated surface than on unmodified glass. It is likely that grafted PDMS forms a fluffy polymer layer in cyclohexane with a distribution of loops and tails, but the structure is presently unknown. So far the properties of PDMS treated glass have not been characterized in detail.

3. Results and Discussion

In Figure 1, the phase diagram of our silica/PDMS/cyclohexane system as described in section 2.1 is presented. Here the polymer packing fraction, ϕ_{pol}, is plotted versus the colloid volume fraction, ϕ_{coll}. The polymer packing fraction is scaled to the overlap concentration, $\phi_{pol} = c/c^*$ with c the weight concentration and c^* its value at overlap. The overlap concentration is calculated by $c^* = M_N/(4/3)\pi R_g^3 N_{Av})$, with N_{Av} Avogadro's number. Some tielines connecting coexisting binodal points are drawn. The critical point is determined by extrapolating the middles of the tielines to the binodal. Our phase diagram is very similar to that of De Hoog et al., who used a slightly larger polymer.[27] The binodal is only slightly tilted compared to that of De Hoog. In the phase diagram, we plotted also the compositions of the samples (A−J) that were used in the wetting experiments.

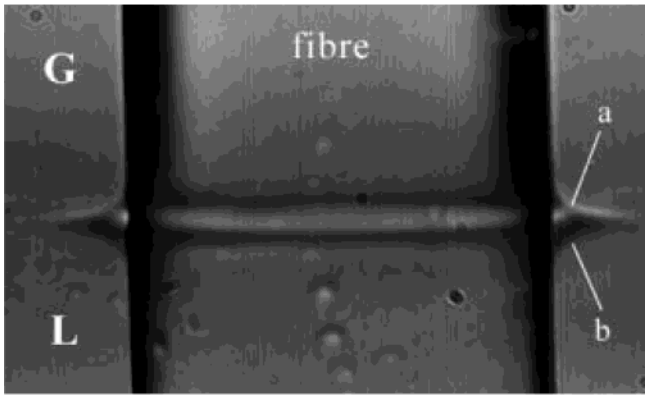

Figure 2. Image of a meniscus at a hard fiber suspended in a colloidal liquid−gas system (sample A). The capital G and L represent the colloidal liquid and the colloidal gas phase, respectively. The meniscus and its mirror image are indicated with a and b, respectively.

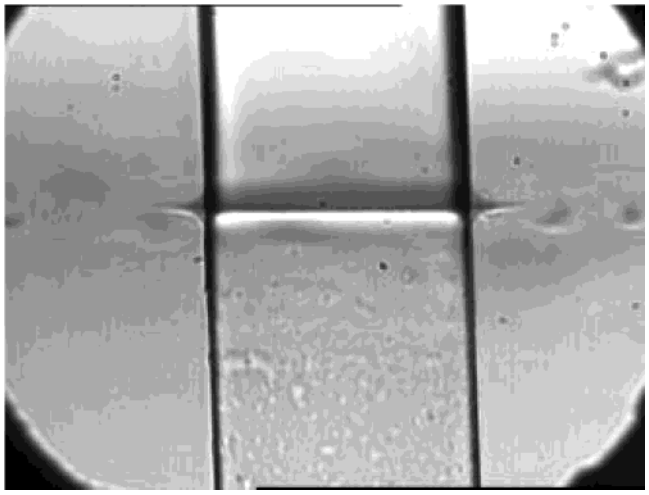

Figure 3. Image of a meniscus at a soft fiber suspended in a colloidal liquid−gas system (sample A).

In Figures 2 and 3, we present some typical images of menisci at the hard and soft fiber for a colloid−polymer composition relatively far from the critical point (sample A, see Figure 1). Such menisci are also observed by Aarts et al. for a planar surface.[20] In both pictures, the colloidal gas and liquid phases are separated by a horizontal interface; the upper phase is the colloidal gas and the lower phase the colloidal liquid. The flat interface itself cannot be seen in these images, but its position can be deduced by means of the mirror images it produces. However, with the naked eye, the interface between the colloidal liquid and gas phase is well visible and very sharp. Near the fiber, we can clearly distinguish the curved part of the meniscus as well as its mirror image. The meniscus can be distinguished from its mirror image by the response to downward or upward movements of the fiber in dynamic experiments. A more detailed

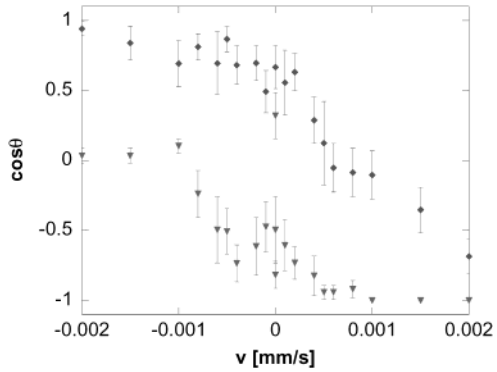

Figure 4. Cosine of the dynamic contact angle of sample A at the substrates as a function of the velocity of the substrate with respect to the colloidal liquid−gas interface. The ◆ are at the hard substrate and ▼ at the soft substrate. A positive velocity corresponds to an advancing contact angle and a negative to a receding contact angle.

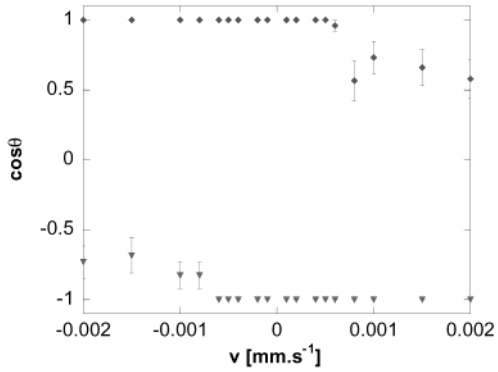

Figure 5. Cosine of the dynamic contact angle of sample J at the substrate as a function of the velocity of the substrate with respect to the colloidal liquid−gas interface. The ◆ are at the hard substrate and ▼ at the soft substrate.

observation of the meniscus shows that there is a bright edge at the meniscus which is not visible at the mirror image. At the hard fiber, the meniscus curves upward for all cases that were examined, whereas at the soft fiber, it curves downward. This implies that the static contact angle is smaller than 90° at the hard fiber and larger than 90° at the soft fiber. This holds for all compositions indicated in Figure 1.

The fact that the static contact angles at the hard fiber are all smaller than 90° implies that the substrate prefers the liquid phase over the gas phase, whereas at the soft fibers, the opposite is true. These qualitative observations can be understood by comparing the interactions between two particles with that between a particle and the substrate. Because the radius of curvature of the fiber is much larger than that of a particle, the fiber can be regarded as a flat substrate. The depletion interaction energy is proportional to the overlap volume of the depletion zones.[2,3] The overlap volume of the depletion zones of a spherical particle, and a flat hard substrate is larger than that of two spherical particles at the same distance, see Figure 6. Hence, the attraction between a particle and the substrate is stronger than that between two particles. In the colloidal liquid phase, there are many more particles than in the colloidal gas phase, so the substrate attracts the colloidal liquid phase much more strongly than the colloidal gas phase. Therefore, a contact angle smaller than 90° is expected at a hard substrate, in agreement with our measurements.

If we attach a fluffy polymer layer at the surface, the depletion attraction is counteracted by a repulsive steric contribution. Such moderated depletion interaction involving a polymer coated surface is called soft depletion.[29−32] It is expected that it will lead to a larger contact angle. We find that the contact angle at the soft fiber is larger than 90° for all colloid−polymer compositions that were examined (Figure 1). The substrate prefers the gas phase over the liquid phase.

The precise value of the static contact angle cannot be easily determined from a static profile. It is very hard to determine the profile because the contour is somewhat fuzzy. Therefore, we determined the static contact angle by interpolation from dynamic contact angles. For sample A (deep in the two phase coexistence region), cos θ is plotted in Figure 4 as a function of the velocity for both substrates. For sample J (closer to the critical point), similar data are plotted in Figure 5. All contact angles were determined by drawing tangents to the liquid−gas interfaces in the three phase points. This leads to an error of about 10° in the data (see error bars). From the plots, it appears that the static advancing and the static receding contact angles are the same, within the error of the experiment. This implies that hysteresis, if any, is smaller than the scatter in the data. The apparent absence of hysteresis may be explained by the fact that colloidal particles are presumably large compared to the typical length scale of the roughness or heterogeneity of the surface. Therefore, such roughness seems to play a minor role in colloidal systems in contrast to what is usually seen for molecular systems. Because of the absence of notable hysteresis, it is justified to determine the static contact angle by interpolation between positive and negative velocities. For the hard substrate, we see for sample A that the static contact angle has a finite value at zero velocity, whereas for sample J, this contact angle is 0° ($\cos\theta_0 = 1$). For this fiber, it can be concluded that sample A is a case of partial wetting and sample J of complete wetting. At the soft fiber, we observe for sample J complete drying and for sample A partial wetting (Figures 4 and 5). So, between these compositions, there must be a transition between partial and complete wetting at the hard fiber and a transition between partial wetting and complete drying at the soft fiber. Static contact angles are measured as described above for all samples A−J indicated in Figure 1. In this way, we were able to narrow down the interval at which the wetting transition occurs. For the samples A−D, we see partial wetting at both substrates. For the samples E−J, we observed complete wetting for the hard substrate and complete drying for the soft substrate. In Figure 1, the complete wetting regime was indicated by the capital C, whereas the capital P corresponds to the partial wetting regime. The wetting transitions occur between the thick tielines, indicated by 2 and 3, in Figure 1. The observation of these wetting transitions is the central result of our paper.

In view of the Cahn argument, we want to present these data as a function of a (reduced) field variable which measures the proximity to the critical point. In ordinary molecular systems, the temperature is the field variable which affects the phase behavior. In colloid-polymer mixtures the polymer reservoir packing fraction, $\phi_{\mathrm{pol}}^{\mathrm{r}}$, is related to the relevant field variable. This quantity plays a role similar to the inverse temperature in molecular systems.[1,4−6,8,9] In theoretical and simulation studies, the phase behavior of colloid-polymer mixtures is often presented in terms of $\phi_{\mathrm{pol}}^{\mathrm{r}}$. However, this quantity is not experimentally accessible. To be able to make some comparison with theoretical predictions,[9,8,11] we have estimated $\phi_{\mathrm{pol}}^{\mathrm{r}}$ by correcting the actual polymer packing fraction (ϕ_{pol}) in the gas phase for the volume of the colloidal particles with their depletion zones by means of scaled particle theory.[5,6] In this estimation, variation of the depletion zone thickness with polymer concentration and particle radius is neglected. A plot

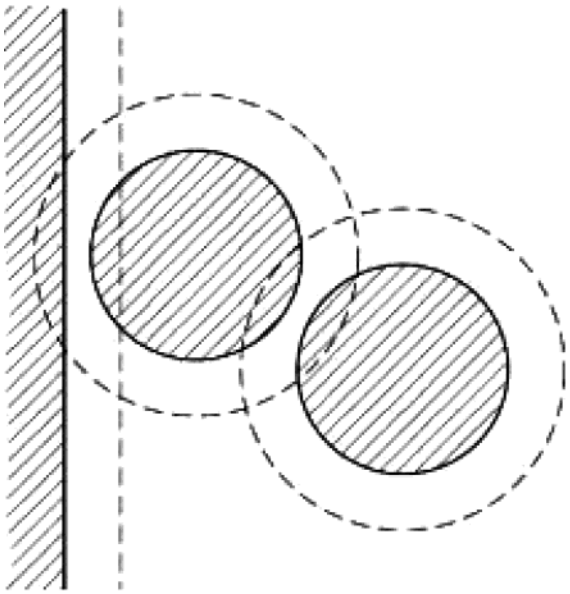

Figure 6. Overlap of depletion zones of 2 particles and of a particle and a wall.

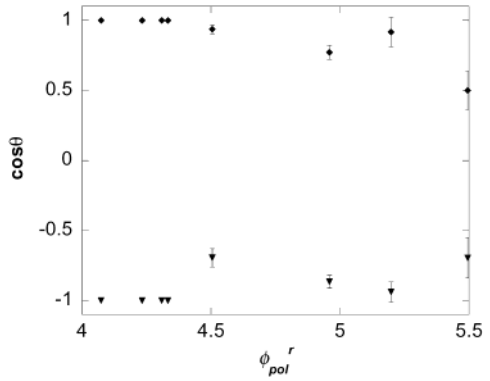

Figure 7. Cosine of the static contact angle as a function of ϕ_{pol}^{r} at the hard substrate (◆) and at the soft substrate (▼).

of cos θ_0 as a function of ϕ_{pol}^{r}, estimated in this way, is shown in Figure 7. The error in cos θ_0 was estimated by taking the root of the average of the squared deviations from the cos θ−velocity plots. From Figure 7, it can be concluded that upon approaching the critical point for both substrates wetting transitions occur in the range $4.3 < \phi_{pol}^{r} < 4.5$. However, near the critical point the polymer reservoir concentration cannot be calculated neither by scaled particle theory nor by other theories. So, for our experimental results, ϕ_{pol}^{r} cannot be used as a measure for the proximity to the critical point. Furthermore, this way to determine the polymer reservoir packing fraction is based on several assumptions.

As an alternative, we will use the difference in colloid volume fraction between the liquid and the gas phase ($\Delta\phi_{coll} = \phi_{coll,l} - \phi_{coll,g}$) to quantify the proximity to the critical point. This quantity can be unambiguously calculated from the experimental data for each composition within the two-phase region, because the tielines are known. Moreover, we know that $\Delta\phi_{coll}$ vanishes in the critical point. It is known that near the critical point for most simple molecular systems $\Delta\phi \sim (T - T_c)^{0.313}$, where T is the temperature and T_c its value in the critical point.[33] If we assume that this critical exponent is also valid for all samples in our system, then $(\Delta\phi_{coll})^{1/0.313}$ would be a quantity proportional to the relevant field variable, at least close to the critical point, and is a suitable measure for the distance to the critical point. In Figure 8, we plot the data accordingly and see that in

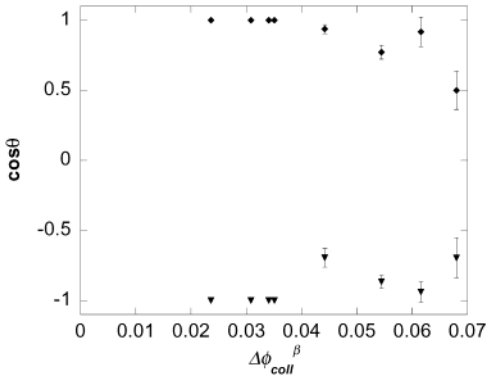

Figure 8. Cosine of the static contact angle as a function of $\Delta\phi_{coll}^{\beta}$ with $\beta = 1/0.313$ at the hard substrate (◆) and at the soft substrate (▼).

the interval $0.034 < (\Delta\phi_{coll})^{1/0.313} < 0.044$ ($0.35 < \Delta\phi_{coll} < 0.38$) cos θ_0 changes between plus unity and a smaller value at the hard fiber and between minus unity and a higher value at the soft fiber. In other words, both the transition from partial to complete wetting at the hard fiber, and that from partial wetting to complete drying at the soft fiber occur in this interval. The occurrence of these wetting transitions is in agreement with the qualitative prediction by Cahn.[15] Between the critical point and the wetting transition point, the hard fiber is completely wet by the colloidal liquid phase, whereas the soft fiber is completely wet by the colloidal gas phase. The fact that both wetting transitions occur in the same range of $\Delta\phi_{coll}$ is probably a coincidence. The position of the wetting transition must depend on surface properties, like the PDMS grafting density. So far, this has not been systematically investigated. The scatter in cos θ_0 at the soft fiber is larger than at the hard fiber. This is probably due to the fact that the treatment of the surface with PDMS is not as reproducible as that with stearyl alcohol. The accuracy of our experimental data is not sufficient to decide whether the wetting transition is first or second order. It seems to be either second order or weakly first order.

We can compare our results quantitatively with predictions from Monte Carlo simulations and density functional theory calculations for similar systems by Dijkstra et al. and Brader et al., respectively.[8,9] In these papers, the location of a wetting transition is calculated for a hard wall and $q = 1$ and 0.6, respectively. In Figure 9, the phase diagram and the wetting transitions from the Monte Carlo simulations, from the density functional theory calculations, and from our experimental results (for which ϕ_{pol}^{r} values were calculated as described above) are plotted together. The liquid−gas binodals are plotted in the $\phi_{pol}^{r} - \phi_{coll}$ representation. The simulated and calculated two phase coexistence regions are at significantly lower ϕ_{pol}^{r} values than our experimental one. These differences may be due to the fact that in the simulations and calculations the polymers are taken to be ideal, whereas in our system, the polymers are swollen and do not behave ideally. For real polymers, around the overlap concentration, the range of the depletion interaction starts to decrease with increasing concentration of polymer. On the other hand, the osmotic pressure, which determines the strength of the attractive force, increases more strongly with concentration than predicted by van't Hoff's law. It turns out that neglecting these effects leads to an over-estimation of the tendency for phase separation: in real systems the binodal is found at much higher values of ϕ_{pol} (or ϕ_{pol}^{r}) than is predicted by the ideal polymer model. Recent calculations by Aarts et al., taking nonideality into account, lead to better, although not perfect, agreement with experiments.[11] This binodal is also

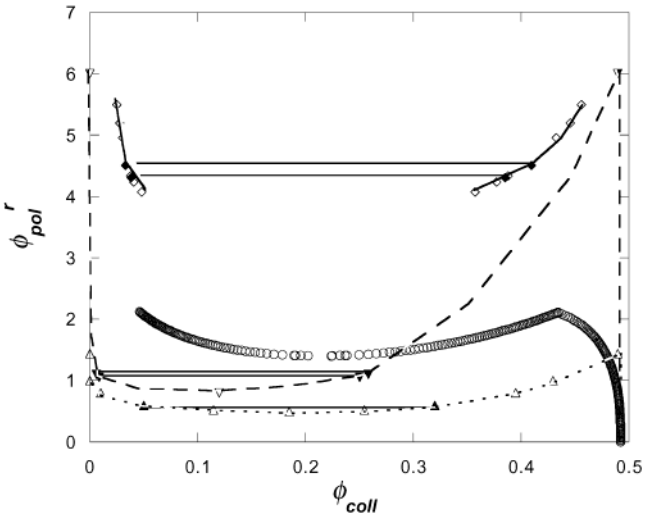

Figure 9. Wetting transitions in the phase diagram for Monte Carlo simulations (▽, dashed curve[8]), density functional calculations (△, dotted curve[9]), and our experiments (◇, solid curve). The locations of the wetting transitions are represented by the solid symbols. The calculations of Aarts are given by ○[11]. Parameters and conditions for each set of data are discussed in the text.

plotted in Figure 9. It is not meaningful to compare the ϕ_{pol}^{r} values at which the wetting transitions occur, because the binodals are significantly different. It was found that the wetting transition occurs somewhere in the regime $0.011 < (\Delta\phi_{coll})^{1/0.313} < 0.012$ and at $(\Delta\phi_{coll})^{1/0.313} = 0.015$ for the simulations and the calculations, respectively. These values are also significantly lower than our results. Brader and Dijkstra observed three layering transitions in the partial wetting regime prior to the transition to complete wetting. These layering transitions cannot be determined experimentally by our method.

4. Conclusions

We have demonstrated that wetting phenomena can be experimentally investigated in colloidal systems exhibiting gas−liquid phase behavior, by independently manipulating the particle−particle interaction and the particle−substrate interaction. The beauty of these systems is that one can effectively eliminate van der Waals forces and replace them with weak attractive interaction of controllable range and strength. This opens up many perspectives for studying the relation between wetting phenomena and the underlying interactions. We observed menisci at fibers far from the critical point and close to criticality and observed the well-known Cahn transition.[15] The adjustment of particle−substrate interactions, being an essential element in such studies, was shown to be possible by means of polymer chains grafted to the substrate. Again, such interactions can be tuned by a judicious choice of chain length and grafting density of the polymer, for which adequate methods are available.[29−32] We have shown that Cahn wetting transitions are present at both a hard and a soft substrate. At the hard substrate, we see a transition from partial to complete wetting. At the soft substrate, we see a transition from partial wetting to complete drying.

References and Notes

(1) Poon, W. C. K.; Pusey, P. N.; Lekkerkerker, H. N. W. *Phys. World* **1996**, *9* (4), 27−32.
(2) Asakura, S.; Oosawa, F. *J. Chem. Phys*. **1954**, *22*, 1255.
(3) Vrij, A. *Pure Appl. Chem*. **1976**, *48*, 471.
(4) Vincent, B.; Edwards, J.; Emmet, S.; Croot, R. *Colloids Surf*. **1988**, *31*, 267−298.
(5) Ilett, S. M.; Poon, W. C. K.; Pusey, P. N. *Phys. Rev. E* **1995**, *51*, 1344−1352.
(6) Lekkerkerker, H. N. W.; Poon, W. C. K.; Pusey, P. N.; Stroobants, A.; Warren, P. B. *Europhys. Lett*. **1992**, *20* (6), 559−564.
(7) Poon, W. C. K. *J. Phys.: Condens. Matter* **2002**, *14*, R859−R880.
(8) Dijkstra, M.; van Roij, R. *Phys. Rev. Lett*. **2002**, *89* (20), 208303−1.
(9) Brader, J. M.; Evans, R.; Schmidt, M.; Öwen, H. *J. Phys.: Condens. Matter* **2002**, *14*, L1−L8.
(10) Wijting, W. K.; Besseling, N. A. M.; Cohen Stuart, M. A. *Phys. Rev. Lett.* **2003**, *90* (19), 196101.
(11) Aarts, D. G. A. L.; Tuinier, R.; Lekkerkerker, H. N. W. *J. Phys.: Condens. Matter* **2002**, *14*, 7551−7561
(12) Young, T. *Philos. Trans*. **1805**, *95*, 69.
(13) Dietrich, S. *Phase Transitions and Critical Phenomena*; Domb, C., Lebowitz, J. L., Eds.; Academic Press: London, 1988; Vol 12.
(14) Schick, M. Introduction to wetting phenomena. *Liquids at interfaces*; Charvolin, J., Joanny, J. F., Zinn-Justin, J., Eds.; Les Houches, Session XLVIII, 1988; Elsevier Publishers: Amsterdam, 1990.
(15) Cahn, J. W. *J. Chem. Phys*. **1977**, *66*, 3667.
(16) de Gennes, P. G. *Rev. Mod. Phys*. **1985**, *57*, 827.
(17) Bonn, D.; Ross, D. Wetting transitions. *Rep. Prog. Phys.* **2001**, *64*, 1085.
(18) Ross, D.; Bonn, D.; Posazhennikova, A. I.; Indekeu, J. O.; Meunier, J. *Phys. Rev. Lett*. **2001**, *87*, 176103.
(19) Bonn, D.; Bertrand, E.; Shahidzadeh, N.; Ragil, K.; Posazhennikova, A. I.; Broseta, D.; Meunier, J.; Indekeu, J. O. *J. Phys.: Condens. Matter* **2001**, *13* (21), 4903−4914.
(20) Aarts, D. G. A. L.; van der Wiel, J. H.; Lekkerkerker, H. N. W. *J. Phys.: Condens. Matter* **2003**, *15*, S245−S250.
(21) van Helden, A. K.; Jansen, J. W.; Vrij, A. *J. Colloid Interface Sci*. **1981**, *81* (2), 354.
(22) Pathmamanoharan, C.; Philipse, A. P. *J. Colloid Interface Sci*. **1994**, *165*, 519−521.
(23) Lyklema, J.; *Fundamentals of Interface and Colloid Science I*; Academic Press: London, 1991; p 4.77.
(24) Kops-Werkhoven, M. M.; Fijnaut, H. M. *J. Chem. Phys*. **1981**, *74*, 1618.
(25) Verhaegh, N. A. M.; van Duijneveldt, J. S.; Dhont, J. K. G.; Lekkerkerker, H. N. W. *Physica A* **1996**, *230*, 409.
(26) Bodnár, I.; Oosterbaan, W. D. *J. Chem. Phys*. **1997**, *106* (18) 7777−7780.
(27) de Hoog, E. H. A.; Lekkerkerker, H. N. W. *J. of Phys. Chem. B* **1999**, *103* (25), 5274−5279.
(28) Fleer, G. J.; Cohen Stuart, M. A.; Scheutjens, J. M. H. M.; Cosgrove, T.; Vincent, B. *Polymers at Interfaces*; Chapman & Hall: Lonodon, 1993.
(29) van Lent, B.; Israels, R.; Scheutjens, J. M. H. M.; Fleer, G. J. *J. Colloid Interface Sci*. **1990**, *137*, 380.
(30) Cosgrove, T.; Heath, T.; van Lent, B.; Leermakers, F. A. M.; Scheutjens, J. M. H. M. *Macromolecules* **1987**, *20*, 1697.
(31) Vincent, B.; Edwards, J.; Emmet, S.; Jones, A. *A. Colloids Surf.* **1986**, *18*, 261.
(32) Jones, A.; Vincent, B. *Colloids Surf*. **1989**, *42*, 113.
(33) Chandler, D.; *Introduction to modern statistical mechanics*; Oxford University Press: New York, 1987.